Available online at www.sciencedirect.com
ScienceDirect
Physica E 35 (2006) 234–240
PHYSICA E
www.elsevier.com/locate/physe

Second-harmonic generation in GaAs-based quantum-cascade lasers

M. Austerer[a,*], S. Schartner[a], C. Pflügl[b], A.M. Andrews[a], T. Roch[a], W. Schrenk[a], G. Strasser[a]

[a]Zentrum für Mikro- und Nanostrukturen, Technische Universität Wien, Floragasse 7, 1040 Vienna, Austria
[b]LabSem, Centro de Estudos em Telecomunicacões, Pontificia Universidade Católica do Rio de Janeiro, Rua Marquês de São Vicente 225, Rio de Janeiro, RJ 22453-900, Brazil

Available online 17 October 2006

Abstract

We report second-harmonic (SH) and sum-frequency generation in GaAs-based quantum-cascade lasers. A doping dependence study of the second-order susceptibility in one of the investigated structure is shown. We also demonstrate that grating-coupled surface emission is a highly efficient way to couple out the SH radiation.

PACS: 42.55.Px; 42.65.Ky

Keywords: Quantum cascade lasers; Nonlinear effects; Semiconductor lasers

1. Introduction

Quantum cascade (QC) lasers are unipolar semiconductor lasers, where the emission wavelength is tailored by bandstructure engineering; for a detailed review on QC lasers see Ref. [1]. Their emission energy is well below the band gaps of the hosting material system. Typical GaAs QC lasers operate in the mid-infrared regime with corresponding energies of ~100 meV, whereas the GaAs band gap is around 1.4 eV. That makes frequency-doubling inside the laser cavity feasible. Such intracavity second-harmonic (SH) generation is not possible in interband semiconductor lasers, where the SH radiation is strongly absorbed. The principle of nonlinear light generation in QC lasers was firstly demonstrated in 2003 [2], since then a lot of progress in this field has been made, such as the improvement of SH generation [3] and the demonstration of third-harmonic generation [4]. A crucial step was the achievement of phase matching [5,6], which was demonstrated by means of modal phase-matching in InP-based QC lasers. Another approach for higher conversion efficiencies is quasi phase-matching by periodically modulating the pump current along the QC laser ridge waveguide [7]. Besides up-conversion, other intracavity nonlinear effects are currently being investigated, such as Raman lasing [8] and anti-stokes [9] emission from QC lasers. The above nonlinear effects are due to higher-order susceptibilities of intersubband transitions. Although InP and GaAs, both of which are commonly used as host materials for QC lasers, have nonzero second-order susceptibilities, there is no resulting second-order polarization in the material for QC lasers. That is due to selection rules for intersubband transitions which allow gain only for TM polarized light, which in turn due to crystal symmetry cannot excite nonlinear polarization in the host material. However it was shown that QC lasers grown on $\langle 1\,1\,1 \rangle$ substrates, show sum-frequency generation due to bulk nonlinearity [10].

Another very interesting topic is intracavity difference-frequency generation in QC lasers. It could eventually be used to generate coherent terahertz radiation in a semiconductor laser at room temperature. Recently THz sideband generation from a THz QC laser and a near-infrared diode laser has been shown [11].

We have investigated SH and sum-frequency generation in three-well and bound-to-continuum GaAs-based QC lasers. The discussed structures are regrowths of structures presented in Refs. [12] and [13], respectively. The SH generation in these samples is due to intersubband

*Corresponding author. Fax: +43 1 58801 36299.
E-mail address: maximilian.austerer@tuwien.ac.at (M. Austerer).

1386-9477/$ - see front matter © 2006 Elsevier B.V. All rights reserved.
doi:10.1016/j.physe.2006.08.015

nonlinearities in the active regions of these devices. The optimization of QC active regions for intracavity SH generation is always jeopardized by the linear absorption that corrupts the laser operation at the fundamental frequency. However, three-well and bound-to-continuum active regions always have higher lying states that can resonantly enhance the second-order susceptibility of the respective QC active region. We show that the linear-to-nonlinear conversion efficiency depends on the doping level in the active region and propose that the optimization of the doping might also lead to improved SH generation. Another issue with intracavity SH generation is the optimization of the waveguide for both fundamental and SH frequencies. We show how a double AlGaAs waveguide helps to improve the conversion efficiency compared to a conventional double-plasmon waveguide as used in GaAs-based QC lasers. We present farfield measurements of the fundamental laser mode and the SH emission that will help investigating modal phase-matching conditions. Furthermore we discuss the use of distributed-feedback (DFB) gratings for single-mode surface emission of SH radiation. This approach has the advantage that only SH light is emitted from the surface of the laser, and no blocking filter for the fundamental radiation is necessary. In this case high-reflective coating of both laser facets is possible and would further enhance the intracavity light intensity and thus the SH output power from the surface.

2. Bandstructure engineering

The bandstructures discussed in this paper for the GaAs/AlGaAs material system are similar to the structures used for the InGaAs/InAlAs system. However the GaAs/AlGaAs system offers the advantage of lattice matching for arbitrary $Al_xGa_{1-x}As$ alloy compositions. The highest Γ-valley conduction band offset can thus be reached for AlAs barriers. AlAs barriers have already been used in the past to improve the performance of QC lasers [14–16].

Our structure A uses AlAs barriers in the active region to design resonant intersubband transitions to generate frequency doubled light [17]. The Γ-valley conduction band edge of structure A together with the moduli squared of the relevant wavefunctions is shown in Fig. 1. The portion shown is similar to a typical three-well [12] QC-active region, but with four AlAs barriers. The AlGaAs barriers in the injector regions have 45% Al content. The wavefunctions are calculated in an effective mass approximation, where band nonparabolicity is taken into account by an energy-dependent effective mass. The lasing transition between levels 3 and 2 is calculated to an energy of 117 meV with a matrix element of $z_{32} = 1.53$ nm. Important nonlinear cascades are the level triplets 2–3–5a, 2–3–5b and 2–3–5c. To estimate the second-order susceptibility all three levels (2,3,5) have to be considered. The transition energies are calculated as follows, $\hbar\omega_{5a3} = 118$ meV ($\hbar\omega_{5a2} = 235$ meV), $\hbar\omega_{5b3} = 120.2$ meV ($\hbar\omega_{5b2} = 237.2$ meV) and $\hbar\omega_{5c3} = 125$ meV ($\hbar\omega_{5c2} = 242$ meV), with the corresponding matrix elements $z_{5a3} = 0.01$ nm ($z_{5a2} = 0.11$ nm),

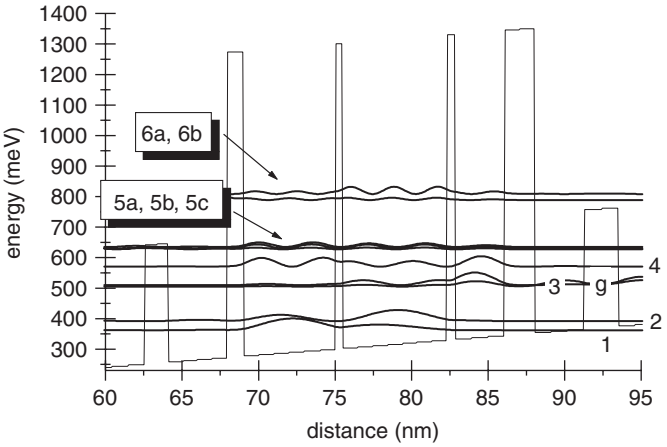

Fig. 1. Conduction band diagram and moduli squared of relevant wavefunctions in the active region of structure A. Important energy levels are labeled "1" through "6" for the active cell and "g" for the injector ground state. The layer thicknesses in nanometers for the GaAs quantum wells and AlAs barriers (italic type) from left to right *1.1*, *6*, *0.5*, *6.8*, *0.5*, *3.3*, *1.9*; the injector bridging regions consist of $GaAs/Al_{0.45}Ga_{0.55}As$ superlattices.

Table 1
Energies and optical matrix elements for relevant transitions in structures A, T and B

	Structure A	Structure T	Structure B
E_{32} (meV)	117	143	124
z_{32} (nm)	1.53	2.09	2.07
$E_{43(5c3)}$ (meV)	128	148	128
$z_{43(5c3)}$ (nm)	0.11	0.22	0.6

For the labelling of the states refer to Figs. 1 and 2. The values depend on the applied electric field across the structure.

$z_{5b3} = 0.05$ nm ($z_{5b2} = 0.11$ nm) and $z_{5c3} = 0.11$ nm ($z_{5c2} = 0.27$ nm) (see Table 1). Further, the energy separation between states 5a, b, c and 6a, b is too large (~165 meV) to contribute essentially to the overall value of χ_2. This is important because the interference between the stages 2–3–5 and 3–5–6 tends to decrease the overall value of χ_2 [3].

Apart from the QC structure with AlAs barriers in the active region, we also investigated active regions with three-well (structure T) and bound-to-continuum (structure B) active regions, where all the barriers consisted of AlGaAs with 45% Al content. The bandstructures and moduli squared of the wavefunctions for these structures are plotted in Fig. 2. The lasing transition takes place between states 3 and 2. The calculated transition energies and matrix elements for structures T and B are given in Table 1. For a detailed description of the laser properties on the fundamental wavelength please refer to Refs. [12] and [13].

For structure T, sum-frequency generation is based on intersubband transitions between states 2–3–4. State 2 and the intermediate state 3 are bound states in the quantum